

Identifying miRNA-mRNA regulation network of chronic pancreatitis based on the significant functional expression

Dan Wang, MD^a, Lei Xin, MD^b, Jin-Huan Lin, MD^a, Zhuan Liao, MD^b, Jun-Tao Ji, MD^a, Ting-Ting Du, MD^a, Fei Jiang, MD^b, Zhao-Shen Li, MD^{b,*}, Liang-Hao Hu, MD^{a,*}

Abstract

Background: The aim of this study was to explore the underlying molecular mechanism and potential molecular biomarkers of chronic pancreatitis (CP) and construct a miRNA-mRNA regulation network.

Methods: To explore the involvement of miRNAs in CP, we downloaded the miRNA and mRNA expression profiles of CP patients and healthy controls and identified the differentially expressed miRNAs and genes. Functional analysis was conducted and significant pathways were utilized. Finally, the miRNA-mRNA regulation network of CP was constructed.

Results: A total of 44 miRNA risk gene pathway relationships were identified, and a complex regulation network was constructed with 3 genes (*ABL1*, *MYC*, and *ANAPC13*) having the highest degree in affecting the network of CP. Importantly, 4 risk genes (*NOTCH3*, *COX5A*, *THBS1*, and *KARS*) and 1 risk miRNA (*hsa-miR-324-5p*) were identified with high prediction accuracy.

Conclusions: In conclusion, we analyzed miRNAs and mRNAs expression profiles in CP, 1 risk miRNA, and 4 risk genes were identified with high prediction accuracy as biomarkers of CP. Although further evaluation in clinical study is needed, our findings provide new insights into the pathogenesis of CP and may improve the diagnosis and therapy by identifying novel targets.

Abbreviations: AUC = area under curve, CP = chronic pancreatitis, DAVID = Visualization and Integrated Discovery, DBTC = dibutyltin dichloride, DEGs = differentially expressed genes, DEmiRs = differentially expressed miRNAs, ECM = extracellular matrix, GSEA = gene set enrichment analysis, HPRD = human protein reference database, PPIs = protein-protein interactions, Sig-pathways = significantly enriched pathways, SP1 = specificity protein 1.

Keywords: biomarker, chronic pancreatitis, diagnosis, miRNA, mRNA, risk gene

1. Introduction

Chronic pancreatitis (CP) is an irreversible disease characterized by progressive inflammation, fibrosis of pancreas, and loss of

pancreatic functions.^[1] Patients may experience abdominal pain and exocrine or endocrine insufficiency. CP is now mainly diagnosed with clinical manifestation and image results. However, CP patients who manifest diabetes, steatorrhea, or obvious atrophic pancreas with pancreatic calculi have progressed to the late stage of the disease. In addition, differential diagnosis between CP and pancreatic cancer is difficult in some cases.^[2] Therefore, an accurate and sensitive diagnostic method of CP is in urgent need.

The pathogenesis process of CP is so far unclear. Recent evidence suggests that risk factors such as alcohol, smoking, genetic or hereditary factors, and autoimmune disease^[3] contribute to the development of CP^[4,5] by modulating endogenous signal pathways such as transforming growth factor (TGF)- β 1 and parathyroid hormone-related protein.^[6] MicroRNAs (miRNAs) were reported to play an important role in the pathogenesis of pancreatic diseases and cumulative evidence indicated that some miRNAs possess the biomarker potential for diagnostic, therapeutic, prognostic exploration of CP.^[7,8] For example, a panel of miRNAs including miR-31 and miR-146a played important roles in the activation of pancreatic stellate cells, which may contribute to pancreatic fibrosis.^[9] Several other miRNAs were supposed to be potentially involved with fibrosis during CP.^[7] Deregulation of the miR-217-SIRT1 pathway promotes epithelial-mesenchymal transition process in pancreatic cancer.^[10] MiR-21, miR-34a, miR-198, and miR-217 were significantly dysregulated in pancreatic ductal adenocarcinoma compared to healthy controls and CP.^[11] Although considerable progress has been made, it is still critical to discover the

Editor: Leonidas G. Koniaris.

DW, LX, and J-HL contributed equally to this work.

The authors report no conflicts of interest.

This study was supported by the National Natural Science Foundation of China (Grant Nos. 81422010 [ZL], 81100316 [LHH], 81470883 [LHH] and 81300355 [LX]), Shanghai ChenGuang Program (Grant No. 12CG40 [LHH]), and Shanghai Rising-Star Program (Grant No. 17QA1405500 [LHH]), and Shanghai Outstanding Youth Doctor Training Program (Grant No. AB83030002015034 [LHH]), and Shanghai Youth Top-notch Talent Program (Grant No. HZW2016FZ67 [LHH]).

Supplemental Digital Content is available for this article.

^a Department of Gastroenterology, ^b Digestive Endoscopy Center, Changhai Hospital, the Second Military Medical University, Shanghai, China.

* Correspondence: Zhao-Shen Li, Department of Gastroenterology, Changhai Hospital, The Second Military Medical University, 168 Changhai Road, Shanghai 200433, China. (e-mail: zhaoshen-li@hotmail.com) and Liang-Hao Hu (e-mail: lianghao-hu@hotmail.com)

Copyright © 2017 the Author(s). Published by Wolters Kluwer Health, Inc. This is an open access article distributed under the Creative Commons Attribution-ShareAlike License 4.0, which allows others to remix, tweak, and build upon the work, even for commercial purposes, as long as the author is credited and the new creations are licensed under the identical terms.

Medicine (2017) 96:21(e6668)

Received: 29 June 2016 / Received in final form: 25 March 2017 / Accepted: 28 March 2017

<http://dx.doi.org/10.1097/MD.0000000000006668>

differentially expressed miRNA and identify the target mRNAs of miRNAs to elucidate the mechanism of miRNA regulation and construct the miRNA-mRNA regulation network of CP.

In the present study, we comprehensively analyzed the miRNA and mRNA expression profiles of patients with CP, and then obtained the risk genes and miRNAs. Subsequently, a complex miRNA-mRNA-pathway regulating network was constructed. Moreover, we compared the miRNAs expression profiles of rat CP model and human CP patients. The common differentially expressed miRNAs and their targets as well as significantly enriched pathways (sig-pathways) were also analyzed.

2. Methods

2.1. MiRNA and mRNA expression profiles of CP

The expression profile of CP was downloaded from Gene Expression Atlas (<http://www.ebi.ac.uk/gxa>)^[12] at European Bioinformatics Institute of the European Molecular Biology Laboratory (EMBL-EBI, <http://www.ebi.ac.uk/>). The expression profile should meet the following condition: organisms (*Homo sapiens*); the samples were extracted from the pancreatic tissues instead of blood or cell lines. Finally, we acquired 2 mRNA expression profiles of CP including E-MEXP-1121 and E-EMBL-6, and 1 miRNA expression profile E-TABM-664. E-MEXP-1121 was about the gene expression of pancreas ductal adenocarcinoma, normal duct cells, tumor stroma, and stroma of CP as well as of several cell lines.^[13] According to our research, we selected 9 CP tissue samples and 9 normal controls from E-MEXP-1121. E-EMBL-6 was the transcription profiling of human normal pancreas samples, and samples from patients with CP, pancreatic cancer, and metastatic pancreatic cancer.^[14] Likewise, 9 CP tissue samples and 9 normal controls were screened for our study. E-TABM-664 was about the microRNA expression patterns to differentiate pancreatic adenocarcinoma from normal pancreas and CP.^[15] In E-TABM-664, 33 CP and 58 normal samples were screened for our study.

2.2. Differentially expressed RNAs

The preprocessing of microarray data included the missing value screening and probe combination for the same gene, where the multiple probe ID would be averaged as a unique value. For the multiple mRNA expression profiles integrated from several studies, the “MetaDE” package^[16] of R/Bioconductor was applied to identify differentially expressed genes (DEGs), and “limma” package^[17] of R/Bioconductor was used to identify differentially expressed miRNAs (DEmiRs) for the single study. The miRNAs or mRNAs with P value $< .05$ were regarded as the DEmiRs or DEGs.

2.3. Identification of miRNAs targets and the risk pathways

The validated miRNA-target interactions were obtained from 3 sources: miRecords,^[18] Tarbase_v6.0,^[19] and miRTarBase.^[20] Using gene set enrichment analysis (GSEA) software, the enriched KEGG pathways (<http://www.genome.jp/kegg/>) were identified based on the mRNA expression profile of CP. Here, default parameters were applied. A pathway was regarded as a risk pathway of CP, only if it was statically significant (enrichment P value $< .1$) in $>50\%$ of all of the datasets related to CP. Besides, we conducted the functional enrichment analysis for the targets of

DEmiRs using the Database for Annotation, Visualization, and Integrated Discovery (DAVID) tool (<http://david.abcc.ncifcrf.gov/>).^[21] Functional enrichment was assessed to be over-represented for Gene Ontology term in biological process category and pathway with P value $< .05$.

2.4. Identification of risk genes

To explore the gene components for risk function deregulation and further provide a bridge to dissect the underlying regulation of the miRNAs, we identified risk genes. Two conditions were required to obtain strict risk genes for CP. First, the genes must be the core risk components of the sig-pathways, which could be obtained by GSEA. Core genes contribute much to the enriched pathway; therefore, the abnormal expression of core genes has great impact on the pathway and biological process. Second, the genes were differentially expressed in CP patients compared with normal controls. Finally, the intersection of core genes and DEGs were considered as the risk genes.

2.5. Detection of risk miRNAs for risk functions

To recognize the significant roles which miRNAs play in the dysfunctions of CP patients, risk miRNAs were identified based on the enrichment of validated miRNA-target genes. We acquired all the genes in sig-pathways that were enriched by the GSEA for the mRNA expression profile of CP.^[22] According to the mRNA, the risk miRNA-mediated pathways were dissected by hypergeometric distribution. Considering the DEmiRs and sig-pathways, the hypergeometric test was used according to the following formula:

$$p_i = 1 - \sum_{t=0}^{x-1} \frac{C_{K_i}^t C_{N-K_i}^{M-t}}{C_N^M}$$

$$(i = 1, 2, \dots, I)$$

Wherein, N is the size of the background genes, K_i is the number of genes targeted by miRNA i , M is the number of genes in pathway A, x is the number of genes in sig-pathway A, which were also targets of DEmiR i , and I is the total number of DEmiRs. The adjusted P values for multiple comparisons were calculated using Benjamini approach. MiRNA-pathway pairs with P value $< .05$ were considered to be in significant relationships.

2.6. MiRNA-mRNA-pathway complex regulation network

We extracted the core genes and DEGs in sig-pathways, which were also targeted by DEmiRs. These genes were considered as the potential risk genes. To explore the potential functional patterns, we study the interactions among risk genes in sig-pathways.^[23] Human Protein Reference Database (HPRD, <http://www.hprd.org/>) is a database of crated proteomic information pertaining to human proteins. Currently, there were 41,327 protein-protein interactions (PPIs) in HPRD. According to our purpose, we extracted the PPIs of human. To systematically investigate the risk pathways mediated by miRNAs, we further proposed a hierarchical model to vertically explore the links among miRNAs, mRNAs, and pathways. By integrating the DEmiR-risk gene relationships, risk gene-pathway pairs, and PPI

of risk genes, the miRNA-mediated pathway crosstalk network was constructed using the Cytoscape software.^[24]

2.7. Microarray analysis of CP rat

We explored the miRNA expression profiles of dibutyltin dichloride (DBTC)-treated CP rat model,^[25] and the Affymetrix miRNA 4.0 experiment and data analysis of the 4 samples (2 CP models and 2 control models) have been completed. Total RNAs were quantified by the NanoDrop ND-2100 (Thermo Scientific) and the RNA integrity was assessed using Agilent 2100 (Agilent Technologies). The sample labeling, microarray hybridization, and washing were performed based on the manufacturer's standard protocols. Briefly, total RNA was tailed with Poly A and then labeled with Biotin. Next, the labeled RNAs were hybridized onto the microarray. After washing and staining the slides, the arrays were scanned by the Affymetrix Scanner 3000 (Affymetrix). Affymetrix GeneChip Command Console software (version 4.0, Affymetrix) was used to analyze array images to get raw data and then offered RMA normalization. Next, Genespring software (version 12.5; Agilent Technologies) was used to process the following data.^[26] Probes that at least 100.0% of samples in any 1 condition of 2 conditions have flags in "P" were chosen for further data analysis. Differentially expressed miRNAs were then identified through fold change as well as *P* value calculated using *t* test. The threshold set for up- and downregulated genes was a fold change ≥ 2.0 and a *P* value $\leq .05$. The study was approved by the Ethics Committee of Shanghai Changhai Hospital. All experiments were performed in accordance with the approved guidelines and regulations, including any relevant details.

3. Results

3.1. Differentially expressed mRNAs and miRNAs in CP patients

By combining the mRNA expression profiles of E-MEXP-1121 and E-EMBL-6, 18 CP samples and 18 normal samples were acquired to study the function of mRNA acting in CP tissues. Besides, 33 CP samples and 58 normal samples were extracted to explore the roles of miRNA in the development of CP. Comparing the CP samples with the normal samples, we acquired 624 DEGs and 305 DEmiRs. Clustering analysis indicated the DEGs and DEmiRs could be differentially expressed between CP and normal samples (Supplementary Figure 1, <http://links.lww.com/MD/B706>).

3.2. Function analysis of genes and miRNAs in CP patients

After the GSEA analysis, a total of 73 downregulated pathways and 84 upregulated pathways were identified (Supplementary Table 1, <http://links.lww.com/MD/B706>) and 40 sig-pathways were acquired (Supplementary Fig. 2A, <http://links.lww.com/MD/B706>). The genes in CP were significantly involved in the extracellular matrix (ECM) receptor interaction, focal adhesion, prion diseases, cell adhesion molecules, and viral myocarditis. Besides, the DEGs closely regulated the processes of vasculature development, cell migration, blood vessel development, and so on (Supplementary Fig. 2B, <http://links.lww.com/MD/B706>).

Subsequently, targets of miRNAs were obtained from the miRecords,^[18] Tarbase_v6.0,^[19] and miRTarBase.^[20] There

were 38,884 interactions including 771 miRNAs and 12,445 target genes in total. For the DEmiRs, 2,246 miRNA-targets were acquired including 78 DEmiRs and 1,990 targets. After the function enrichment for the targets of DEmiRs, it came out that these DEmiRs mainly regulated Pathways in cancer, selenoamino acid metabolism, ribosome, and p53 signaling pathway (Supplementary Fig. 2C, <http://links.lww.com/MD/B706>). Meanwhile, DEmiRs targeted genes mediating the regulation of protein metabolic process, RNA metabolic process, cell cycle, and so on (Supplementary Fig. 2D, <http://links.lww.com/MD/B706>).

Besides, by integrating analysis of mRNA and miRNA expression profiles, we found that 142 targets were differentially expressed, which were targeted by 27 DEmiRs and consisted of 166 DEmiR-DEG pairs. In the 166 DEmiR-DEG pairs, 76 pairs downregulated and 90 pairs upregulated the target genes (Supplementary Table 2, <http://links.lww.com/MD/B706>). Functions of these differentially expressed targets were also analyzed, and the results showed that DEGs targeted by DEmiRs played roles in the cellular macromolecule metabolic process, macromolecule biosynthetic process, anatomical structure formation of morphogenesis, and so on (Supplementary Fig. 3, <http://links.lww.com/MD/B706>).

3.3. MiRNA-pathway pairs

In the sig-pathways, we acquired 629 core genes including 161 differentially expressed core genes and 468 nondifferentially expressed core genes, 879 noncore genes including 17 differentially expressed noncore genes, and 862 nondifferentially expressed noncore genes (Fig. 1A). Besides, 629 core genes included 89 upregulated DEGs and 72 downregulated DEGs (Fig. 1B). Through the hypergenomic test, we acquired 33 miRNA-pathway pairs consisted of 21 DEmiRs and 17 pathways (Table 1). A total of 44 DEmiR-risk gene-pathway relationships were acquired including 12 DEmiRs, 21 risk genes, and 16 sig-pathways (Fig. 2).

3.4. Analysis of miRNA-mRNA-pathway regulation network

As mapping to the PPI network of HPRD database, 335 PPIs of risk genes were extracted. Combining the PPIs of risk genes and relationships among DEmiRs, risk genes, and pathways, we constructed the DEmiR-risk gene-pathway regulation network (Fig. 3). The PPI network was a scale-free network and the hub nodes would be explored according to the topological characteristics. The network topological characteristics of whole network included betweenness centrality, closeness centrality, average cluster coefficient, degree, average shortest path length, and topological coefficient (Supplementary Fig. 4, <http://links.lww.com/MD/B706>). In the complex network, there were 26 DEmiR-risk gene pairs, and 9 DEmiRs and risk genes in 26 DEmiR-risk gene pairs had the opposite expression trend. DEmiRs and risk genes in the rest of 17 DEmiR-risk gene pairs had the same expression tendency. For example, hsa-miR-324-5p was upregulated in the CP patients, and potentially targeted RPL27, ANAPC13, ATP5H, COX5A, and COL6A1. These genes were risk genes and differentially expressed in CP, further activated the pathways of ubiquitin-mediated proteolysis, ribosome, Parkinson disease, Huntington disease, oxidative phosphorylation, focal adhesion, and ECM receptor interaction (Fig. 3). COX5A was putatively targeted by hsa-miR-484 and hsa-miR-324-5p. Meanwhile, COX5A was downregulated in CP and was a core gene in the pathways of Parkinson disease, Huntington disease,

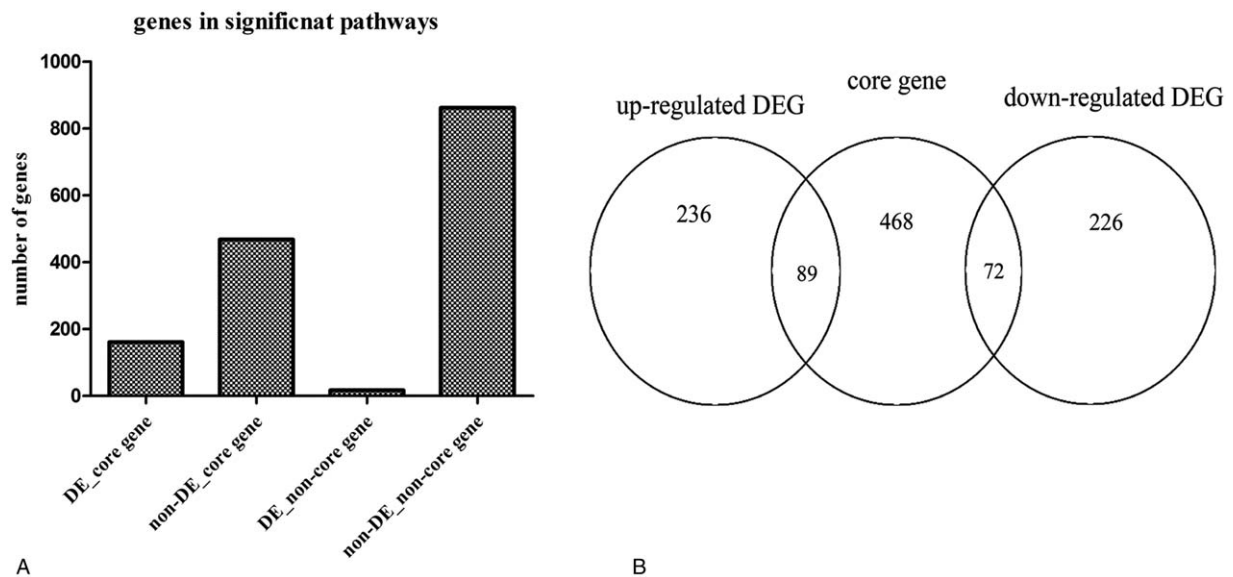


Figure 1. (A) The core genes in the significantly enriched pathways. (B) The number of different types of genes in sig-pathways. The relationship core genes and DEGs, DE=differentially express, DEG=differentially expressed gene.

Alzheimer disease, oxidative phosphorylation, and cardiac muscle contraction (Figs. 2 and 3). NOTCH3 was another potential biomarker and an upregulated core gene in the risk pathway of dorsoventral axis formation (Figs. 2 and 3). Besides,

Table 1
The significant miRNA-pathways pairs.

miRNA	Pathway
hsa-miR-106b	Ubiquitin-mediated proteolysis
hsa-miR-128b	Dorso-ventral-axis formation
hsa-miR-133b	Dorso-ventral-axis formation
hsa-miR-135b	Regulation of actin cytoskeleton
hsa-miR-143	Dorso-ventral-axis formation
hsa-miR-184	FC gamma R-mediated Phagocytosis
hsa-miR-195	Viral myocarditis
hsa-miR-195	Focal adhesion
hsa-miR-199b	ECM receptor interaction
hsa-miR-199b	Focal adhesion
hsa-miR-203	Viral myocarditis
hsa-miR-206	Dorso-ventral-axis formation
hsa-miR-21	TGF beta signaling pathway
hsa-miR-214	Focal adhesion
hsa-miR-30e	Ubiquitin-mediated proteolysis
hsa-miR-328	ECM receptor interaction
hsa-miR-34b	Dorso-ventral-axis formation
hsa-miR-34c	Dorso-ventral-axis formation
hsa-miR-377	FC-gamma-R-mediated phagocytosis
hsa-miR-377	Regulation of actin cytoskeleton
hsa-miR-377	Focal adhesion
hsa-miR-409-3p	Complement and coagulation cascades
hsa-miR-409-3p	Type I diabetes mellitus
hsa-miR-409-3p	Regulation of autophagy
hsa-miR-409-3p	Graft versus host disease
hsa-miR-409-3p	Proteasome
hsa-miR-409-3p	Allograft rejection
hsa-miR-409-3p	Leishmania infection
hsa-miR-409-3p	Systemic lupus erythematosus
hsa-miR-424	Viral myocarditis
hsa-miR-424	Focal adhesion
hsa-miR-485-3p	Antigen processing and presentation
hsa-miR-520c	ECM receptor interaction

there were 3 upregulated DEmiRs in the CP putatively targeted NOTCH3, which were hsa-miR-206, hsa-miR-34c, and hsa-miR-484.

Moreover, we extracted topological properties of the risk genes in whole PPI network (Table 2), and found 3 genes with highest degrees (*ABL1*, *MYC* and *ANAPC13*) comparing with other risk genes (Table 2). These 3 genes affected more genes than other risk genes and may also play more important roles than other risk genes in the occurrence of CP.

With the 5-fold cross-validation, we assessed the prediction accuracy of DEmiRs and risk genes in the complex network (Table 3). The highest prediction accuracy miRNA was hsa-miR-324-5p, and the area under curve (AUC) was 0.871. Besides, 4 genes had the AUC >0.90, which were *NOTCH3*, *COX5A*, *THBS1*, and *KARS* (Fig. 4A). Moreover, the AUCs of *ABL1*, *MYC*, and *ANAPC13*, which ranked highest degree in the PPI network, were 0.8519, 0.8086, and 0.8981 (Tables 2 and 3). As to the expression level, the results showed that hsa-miR-324-5p, *NOTCH3*, and *THBS1* were upregulated in the CP, whereas *COX5A* and *KARS* were downregulated in the CP (Fig. 4B). The higher prediction accuracy of hsa-miR-324-5p and *COX5A* showed that they may function as a motif to promote the development of CP.

3.5. Comparing the differentially expressed miRNAs of rat and human

To explore whether the miRNA expression profile of rat CP model is similar with our analysis results in human CP patients, further comparison of the miRNA expression profiles of the 2 species was performed. A total of 137 DEmiRs were acquired in rat models including 4 downregulated miRNAs and 133 upregulated miRNAs (Supplementary Figure 5, <http://links.lww.com/MD/B706>). There were 4 DEmiRs shared by both homo and rat including miR-182, miR-184, miR-205, and miR-431. All of the 4 miRNAs were upregulated both in homo and rat.

Target genes of DEmiRs were the intersection predicted with 2 databases (Targetscan, microRNAorg). GO analysis and KEGG

Table 2**The network topological properties of risk genes in the PPI network.**

Gene	Average shortest path length	Betweenness centrality	Closeness centrality	Clustering coefficient	Degree	Topological coefficient
<i>ABL1</i>	2.9724	0.01202	0.3364	0.0575	108	0.0206
<i>MYC</i>	3.1510	0.00461	0.3174	0.0576	70	0.0277
<i>TGFBR2</i>	3.3223	0.00129	0.3010	0.1063	36	0.0419
<i>THBS1</i>	3.7419	0.00140	0.2672	0.0739	35	0.0474
<i>RP5</i>	3.6486	0.00052	0.2741	0.0286	15	0.0783
<i>NOTCH3</i>	3.8098	0.00007	0.2625	0.0606	12	0.1145
<i>MRE11A</i>	3.7506	0.00007	0.2666	0.2182	11	0.1096
<i>CCND2</i>	3.6933	0.00008	0.2708	0.1111	10	0.1225
<i>UBA2</i>	4.0126	0.00004	0.2492	0.1429	8	0.1612
<i>KARS</i>	3.9415	0.00005	0.2537	0.0357	8	0.1285
<i>NEO1</i>	4.1089	0.00024	0.2434	0	4	0.2615
<i>COL6A1</i>	4.5962	0.00001	0.2176	0.1667	4	0.2663
<i>MPZL1</i>	3.7850	0.00010	0.2642	0.3333	3	0.3778
<i>COX5A</i>	4.2331	0.00019	0.2362	0	3	0.3333
<i>NARS</i>	4.0340	3.903E-05	0.2479	0	2	0.5
<i>UBE2J1</i>	4.5916	0	0.2178	0	1	0
<i>ATP5H</i>	4.6946	0	0.2130	0	1	0

PPIs = protein-protein interactions.

Table 3**The expression level and ROC curve for the RNAs in DEmiR-risk gene-pathway relationships.**

miRNA	logFC	t Test	P	ROC	PMID
hsa-miR-324-5p	1.2993	6.3380	2.34E-10	0.871	
hsa-miR-34c	1.0903	5.3182	1.05E-07	0.7769	
hsa-miR-484	0.8689	4.2386	2.25E-05	0.749	23697990
hsa-miR-206	0.8469	4.1313	3.61E-05	0.7236	
hsa-miR-429	0.7488	3.6523	2.60E-04	0.7202	
hsa-miR-346	0.7186	3.5054	4.56E-04	0.7066	
hsa-miR-203	0.8533	4.1622	3.16E-05	0.6891	20652642
hsa-let-7b	0.8506	4.1492	3.34E-05	0.6813	23684747
hsa-miR-155	0.4866	2.3734	1.76E-02	0.6742	25520858;22504911
hsa-miR-21	0.7179	3.5017	4.63E-04	0.6688	25908274;24464300
hsa-miR-107	0.6537	3.1887	1.43E-03	0.6426	
hsa-miR-375	0.5925	2.8903	3.85E-03	0.5384	24575833
NOTCH3	1.4740	4.5636	5.03E-06	0.9444	18069660
COX5A	-1.3299	-4.1173	3.83E-05	0.9444	
THBS1	1.2575	3.8934	9.89E-05	0.9321	25393578;24571389; 16181801
KARS	-1.0526	-3.2589	1.12E-03	0.9167	
ANAPC13	-1.3182	-4.0812	4.48E-05	0.8981	
THBS2	1.2225	3.7848	1.54E-04	0.892	
UBA2	-1.2316	-3.8131	1.37E-04	0.8827	
TGFBR2	1.3251	4.1026	4.09E-05	0.8796	19625278
COL6A1	1.2738	3.9437	8.02E-05	0.8796	
GGT5	1.0626	3.2898	1.00E-03	0.8673	
RPL5	-1.1768	-3.6434	2.69E-04	0.8673	
CCND2	1.1343	3.5119	4.45E-04	0.8611	
ABL1	1.1813	3.6574	2.55E-04	0.8519	
NARS	-1.1609	-3.5942	3.25E-04	0.8488	
UBE2J1	-1.1848	-3.6681	2.44E-04	0.8488	
RPL27	-1.0788	-3.3401	8.37E-04	0.8426	
INPP5D	1.1435	3.5403	4.00E-04	0.8333	
NEO1	1.0351	3.2046	1.35E-03	0.8302	
ATP5H	-1.1098	-3.4360	5.91E-04	0.8302	
PSEN2	-1.0923	-3.3818	7.20E-04	0.8241	
MRE11A	-1.1061	-3.4247	6.16E-04	0.821	
MYC	1.0076	3.1196	1.81E-03	0.8086	17496331
ATP5J	-1.0121	-3.1334	1.73E-03	0.8025	
MPZL	1.0376	3.2125	1.32E-03	0.7809	

DEmiR = differentially expressed miRNAs, ROC = receiver-operating characteristic.

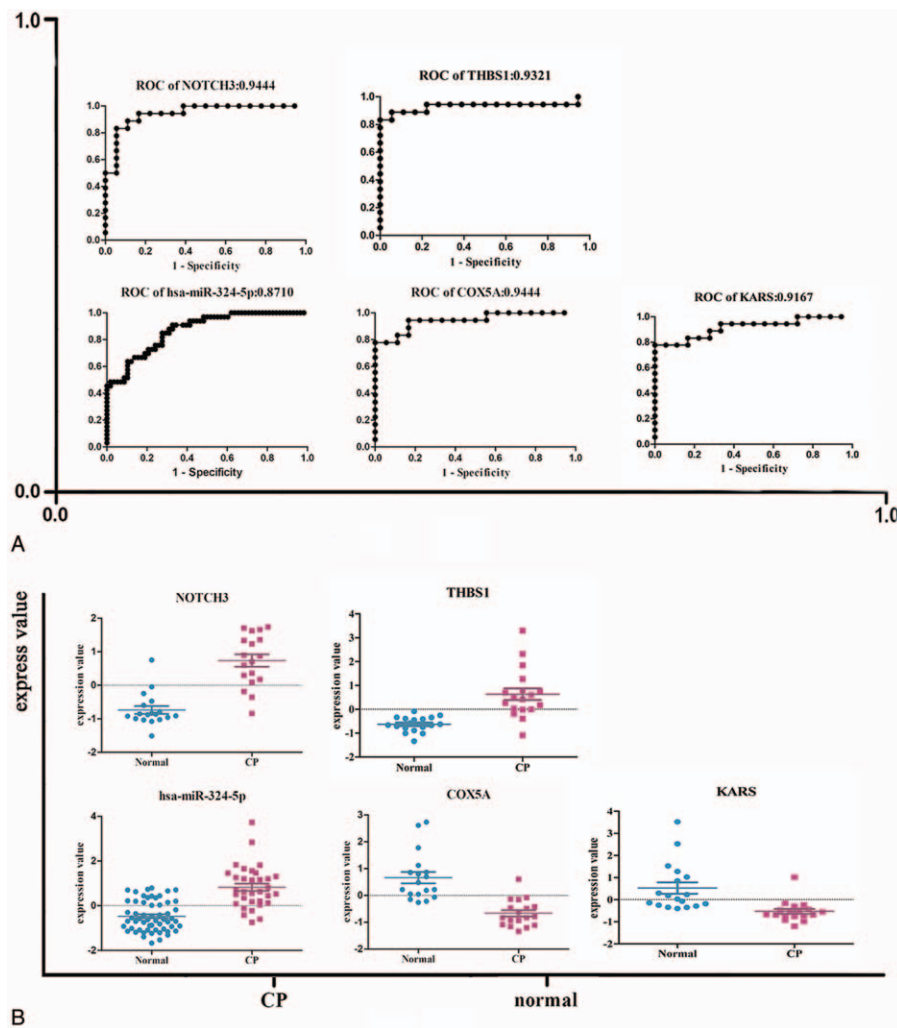


Figure 4. (A) Expression level and receiver-operating characteristic curve (ROC) curve for the potential biomarkers. (B) The expression level of hsa-miR-324-5p, NOTCH3, COX5A, THBS1, and KARS. The ROC curve of hsa-miR-324-5p, NOTCH3, COX5A, THBS1, and KARS.

4. Discussion

In this study, we analyzed the mRNA and miRNA expression profiles of patients with CP. The risk miRNA-gene-pathway relationships were identified including 12 risk DE miRs, 21 risk genes, and 16 risk pathways. Twenty-one risk genes targeted by DE miRs were acquired and were also differentially expressed in CP. Subsequently, a complex PPI regulation network was constructed. Three genes (*ABL1*, *MYC*, and *ANAPC13*) which had the highest degrees in the PPI network may play important roles in the occurrence of CP. Among the risk miRNAs, hsa-miR-324-5p had the highest prediction accuracy (0.8710) and was the potential biomarker of CP. Four of these risk genes (*NOTCH3*, *COX5A*, *THBS1*, and *KARS*) showing high prediction accuracy were the candidate biomarkers of CP. Moreover, we compared the miRNA expression profiles of rat and homo. Four common DE miRs (miR-182, -184, -205, and -431) were obtained which were involved in MAPK signaling pathway etc.

In our study, 12 risk miRNAs were identified, and 7 miRNAs of them have been proved to be associated with CP or pancreatic cancer. Most of these risk miRNAs were very potentially involved in fibrosis. For example, miR-484 may regulate IL-8 expres-

sion,^[27] and thus is associated with fibrosis.^[28] MiR-34c could target notch signaling pathway^[29]; moreover, miR-34c attenuates epithelial-mesenchymal transition and kidney fibrosis of mice^[30] and may target acyl-CoA synthetase long-chain family member 1 gene associated with hepatic fibrosis.^[31] MiR-324-5p was presented to directly target specificity protein 1 (SP1) and E26 transformation-specific 1, which play important roles in ECM signaling pathway by modulating MMP2 and MMP9 expression and activity.^[32] Moreover, transcription factor SP1 plays an important role in fibrosis by mediating the expression of a variety of fibrotic genes expression. Inhibition of SP1 with decoy ODN, a potent inhibitor of SP1-activated transcription, was reported to be a potential effective approach to prevent the progression of hepatic fibrosis.^[33] Therefore, miR-324-5p may directly target SP1 to prevent fibrosis. Furthermore, miR-324-5p is associated with NF- κ B signaling pathway and thus regulates fibrosis and inflammation.^[34] More importantly, in our results, hsa-miR-324-5p had the highest prediction and was the potential biomarker of CP. In the complex risk miRNA-mRNA-pathway network constructed in our study, hsa-miR-324-5p putatively targeted *COX5A* to regulate oxidative phosphorylation,^[35] and may bind *ANAPC13* to modulate ubiquitin-mediated-

proteolysis; moreover, hsa-miR-324-5p may also get involved in ECM-receptor-interaction and focal-adhesion pathways putatively through COL6A1 gene, which is consistent with previous reports. Our findings suggested a possible molecular mechanism for CP pathogenesis.

Several proved signaling pathways were also displayed in our risk miRNA-mRNA-pathway regulating network, such as TGF- β signaling pathway, ECM signaling pathway, dorso-ventral-axis formation pathway, WNT/ β -catenin signaling pathway, ubiquitin-mediated proteolysis pathway, and oxidative phosphorylation pathway. Biomolecular pathways involved in protein degradation-related pathways (lysosome, ubiquitin-mediated proteolysis, and the proteasome) were associated with the conversion of quiescent to activated pancreatic stellate cells, which is a significant event in the development of CP.^[9]

Among the risk genes, we found that COX5A is involved in oxidative phosphorylation pathway among others; THBS1 is associated with ECM-receptor-interaction, focal adhesion, and TGF- β signaling pathway^[36]; KARS is correlated with aminoacyl-tRNA-biosynthesis. We also found that miR-484, -206, and -34c putatively target NOTCH3 gene, thereby got involved in dorso-ventral-axis formation pathway. NOTCH3 is a critical factor in WNT/ β -catenin signaling pathway and is also implicated in TGF- β signaling pathway associated with epithelial-mesenchymal transition.^[37] NOTCH3 is directly associated with fibrosis.^[38,39] It is markedly upregulated in fibrotic liver tissue, and may regulate the activation of hepatic stellate cells; moreover, selective inhibition of NOTCH3 prevents the hepatic fibrosis process.^[40] In addition, NOTCH3 is related to the occurrence of hypertension renal fibrosis.^[40,41] NOTCH3 expression is also reported to be elevated in the ducts of CP.^[42] Therefore, NOTCH3 and the other 3 risk genes may be promising risk biomarkers of CP, which need further confirmation in clinical study.

We also compared the miRNA expression profile of rats and homo. Only 4 common DE miRNAs were identified both upregulated in the 2 species. On one hand, the limited number of CP model limited the accuracy of results. On the other hand, DBTC also damages other organs such as liver while inducing fibrosis in pancreas.^[43–45] Therefore, the pathology of DBTC-induced CP onset may be different from clinical onset of CP. As the miRNA expression profile of this rat CP model had only 4 shared DE miRNAs with homo; this DBTC-treated rat CP model may not suitability for miRNA expression pattern investigation of CP.

In conclusion, we analyzed miRNAs and mRNAs expression profiles in CP, 1 risk miRNA, and 4 risk genes were identified with high prediction accuracy being as biomarkers of CP. However, further confirmation in clinical study is needed. Our findings provide new insights into the mechanisms of CP pathogenesis and may improve the diagnosis and therapy of the disease by identifying novel targets.

References

- Braganza JM, Lee SH, McCloy RF, et al. Chronic pancreatitis. *Lancet* 2011;377:1184–97.
- Ruszniewski P, Malka D, Hammel P, et al. The diagnostic dilemmas in discrimination between pancreatic carcinoma and chronic pancreatitis. *Gut* 2004;53:771.
- Coté GA, Yadav D, Slivka A, et al. Alcohol and smoking as risk factors in an epidemiology study of patients with chronic pancreatitis. *Clin Gastroenterol Hepatol* 2011;9:266–73. quiz e227.
- Conwell DL, Lee LS, Yadav D, et al. American Pancreatic Association Practice Guidelines in Chronic Pancreatitis: evidence-based report on diagnostic guidelines. *Pancreas* 2014;43:1143–62.
- Aghdassi AA, Weiss FU, Mayerle J, et al. Genetic susceptibility factors for alcohol-induced chronic pancreatitis. *Pancreatology* 2015;15:S23–31.
- Falzon M, Bhatia V. Role of parathyroid hormone-related protein signaling in chronic pancreatitis. *Cancers* 2015;7:1091–108.
- Hu LH, Ji JT, Li ZS. Potential application of miRNAs as diagnostic and therapeutic tools in chronic pancreatitis. *J Cell Mol Med* 2015;19:2049–57.
- Xin L, Gao J, Wang D, et al. Novel blood-based microRNA biomarker panel for early diagnosis of chronic pancreatitis. *Sci Rep* 2017;7:40019.
- Masamune A, Nakano E, Hamada S, et al. Alteration of the microRNA expression profile during the activation of pancreatic stellate cells. *Scand J Gastroenterol* 2014;49:323–31.
- Deng S, Zhu S, Wang B, et al. Chronic pancreatitis and pancreatic cancer demonstrate active epithelial-mesenchymal transition profile, regulated by miR-217-SIRT1 pathway. *Cancer Lett* 2014;355:184–91.
- Vychytilova-Faltejskova P, Kiss I, Klusova S, et al. MiR-21, miR-34a, miR-198 and miR-217 as diagnostic and prognostic biomarkers for chronic pancreatitis and pancreatic ductal adenocarcinoma. *Diagnost Pathol* 2015;10:38.
- Kapushesky M, Emam I, Holloway E, et al. Gene expression atlas of the European bioinformatics institute. *Nucleic Acids Res* 2010;38:D690–698.
- Pilarsky C, Ammerpohl O, Sipos B, et al. Activation of Wnt signalling in stroma from pancreatic cancer identified by gene expression profiling. *J Cell Mol Med* 2008;12:2823–35.
- Abdollahi A, Schwager C, Kleeff J, et al. Transcriptional network governing the angiogenic switch in human pancreatic cancer. *Proc Natl Acad Sci U S A* 2007;104:12890–5.
- Bloomston M, Frankel WL, Petrocra F, et al. MicroRNA expression patterns to differentiate pancreatic adenocarcinoma from normal pancreas and chronic pancreatitis. *JAMA* 2007;297:1901–8.
- Wang X, Kang DD, Shen K, et al. An R package suite for microarray meta-analysis in quality control, differentially expressed gene analysis and pathway enrichment detection. *Bioinformatics* 2012;28:2534–6.
- Smyth GK. Linear models and empirical bayes methods for assessing differential expression in microarray experiments. *Stat Appl Genet Mol Biol* 2004;3: Article3.
- Xiao F, Zuo Z, Cai G, et al. Li T. miRecords: an integrated resource for microRNA-target interactions. *Nucleic Acids Res* 2009;37:D105–110.
- Sethupathy P, Corda B, Hatzigeorgiou AG. TarBase: A comprehensive database of experimentally supported animal microRNA targets. *Rna* 2006;12:192–7.
- Hsu SD, Lin FM, Wu WY, et al. miRTarBase: a database curates experimentally validated microRNA-target interactions. *Nucleic Acids Res* 2011;39:D163–169.
- Dennis GJR, Sherman BT, Hosack DA, et al. DAVID: Database for Annotation, Visualization, and Integrated Discovery. *Genome Biol* 2003;4:3.
- Subramanian A, Tamayo P, Mootha VK, et al. Gene set enrichment analysis: a knowledge-based approach for interpreting genome-wide expression profiles. *Proc Natl Acad Sci U S A* 2005;102:15545–50.
- Frampton AE, Castellano L, Colombo T, et al. Integrated molecular analysis to investigate the role of microRNAs in pancreatic tumour growth and progression. *Lancet* 2015;385(Suppl 1):S37.
- Shannon P, Markiel A, Ozier E, et al. Cytoscape: a software environment for integrated models of biomolecular interaction networks. *Genome Res* 2003;13:2498–504.
- Lerch MM, Gorelick FS. Models of acute and chronic pancreatitis. *Gastroenterology* 2013;144:1180–93.
- Knapen D, Vergauwen L, Laukens K, et al. Best practices for hybridization design in two-colour microarray analysis. *Trends Biotechnol* 2009;27:406–14.
- Mei Q, Xue G, Li X, et al. Methylation-induced loss of miR-484 in microsatellite-unstable colorectal cancer promotes both viability and IL-8 production via CD137L. *J Pathol* 2015;236:165–74.
- Bhattacharyya S, Gutti U, Mercado J, et al. MAPK signaling pathways regulate IL-8 mRNA stability and IL-8 protein expression in cystic fibrosis lung epithelial cell lines. *Am J Physiol Lung Cell Mol Physiol* 2011;300:L81–7.
- Liu XD, Zhang LY, Zhu TC, et al. Overexpression of miR-34c inhibits high glucose-induced apoptosis in podocytes by targeting Notch signaling pathways. *Int J Clin Exp Pathol* 2015;8:4525–34.
- Morizane R, Fujii S, Monkawa T, et al. miR-34c attenuates epithelial-mesenchymal transition and kidney fibrosis with ureteral obstruction. *Sci Rep* 2014;4:4578.
- Li WQ, Chen C, Xu MD, et al. The rno-miR-34 family is upregulated and targets ACSL1 in dimethylnitrosamine-induced hepatic fibrosis in rats. *FEBS J* 2011;278:1522–32.

- [32] Cao L, Xie B, Yang X, et al. MiR-324-5p suppresses hepatocellular carcinoma cell invasion by counteracting ECM degradation through post-transcriptionally downregulating ETS1 and SP1. *PloS One* 2015;10: e0133074.
- [33] Chen H, Zhou Y, Chen KQ, et al. Anti-fibrotic effects via regulation of transcription factor Sp1 on hepatic stellate cells. *Cell Physiol Biochem* 2012;29:51–60.
- [34] Song L, Liu D, Zhao Y, et al. Sinomenine inhibits breast cancer cell invasion and migration by suppressing NF-kappaB activation mediated by IL-4/miR-324-5p/CUEDC2 axis. *Biochem Biophys Res Commun* 2015;464:705–10.
- [35] Barrow JJ, Balsa E, Verdeguer F, et al. Bromodomain inhibitors correct bioenergetic deficiency caused by mitochondrial disease complex i mutations. *Mol Cell* 2016;64:163–75.
- [36] Benzoubir N, Lejamtel C, Battaglia S, et al. HCV core-mediated activation of latent TGF-beta via thrombospondin drives the crosstalk between hepatocytes and stromal environment. *J Hepatol* 2013;59: 1160–8.
- [37] Liu L, Chen X, Wang Y, et al. Notch3 is important for TGF-beta-induced epithelial-mesenchymal transition in non-small cell lung cancer bone metastasis by regulating ZEB-1. *Cancer Gene Ther* 2014;21:364–72.
- [38] Djudjaj S, Chatziantoniou C, Raffetseder U, et al. Notch-3 receptor activation drives inflammation and fibrosis following tubulointerstitial kidney injury. *J Pathol* 2012;228:286–99.
- [39] Lai JM, Zhang X, Liu FF, et al. Redox-sensitive MAPK and Notch3 regulate fibroblast differentiation and activation: a dual role of ERK1/2. *Oncotarget* 2016;7:43731–45.
- [40] Chen YX, Weng ZH, Zhang SL. Notch3 regulates the activation of hepatic stellate cells. *World J Gastroenterol* 2012;18:1397–403.
- [41] Xu H, Zhang J, Zheng L, et al. Expression of Notch3 and hypertensive renal fibrosis. *Zhong Nan Da Xue Xue Bao Yi Xue Ban* 2013;38: 1130–4.
- [42] Bhanot U, Kohntop R, Hasel C, et al. Evidence of Notch pathway activation in the ectatic ducts of chronic pancreatitis. *J Pathol* 2008; 214:312–9.
- [43] Zhao HF, Ito T, Gibo J, et al. Anti-monocyte chemoattractant protein 1 gene therapy attenuates experimental chronic pancreatitis induced by dibutyltin dichloride in rats. *Gut* 2005;54:1759–67.
- [44] Glawe C, Emmrich J, Sparmann G, et al. In vivo characterization of developing chronic pancreatitis in rats. *Lab Invest* 2005;85:193–204.
- [45] Aghdassi AA, Mayerle J, Christochowitz S, et al. Animal models for investigating chronic pancreatitis. *Fibrogenesis Tissue Repair* 2011;4:26.